Synthesis and Electrochemistry of Electronegative Spiroannelated Methanofullerenes: Theoretical Underpinning of the Electronic Effect of Addends and a Reductive Cyclopropane Ring-Opening Reaction

Brian Knight,[†] Nazario Martín,*[,‡] Toshinobu Ohno,[†] Enrique Ortí,[§] Concepció Rovira,[||] Jaume Veciana,[||] José Vidal-Gancedo,[||] Pedro Viruela,[§] Rafael Viruela,[§] and Fred Wudl*[,†]

Contribution from the Institute for Polymers and Organic Solids, Departments of Physics and Chemistry, University of California, Santa Barbara, California 93106, Departamento de Química Orgánica, Facultad de Química, Universidad Complutense, E-28040 Madrid, Spain, Departamento de Química Física, Universidad de Valencia, E-46100 Burjassot (Valencia), Spain, and Institut de Ciència de Materials de Barcelona (CSIC), Campus U.A.B., E-08193 Bellaterra, Spain

Received July 5, 1996[⊗]

Abstract: Spiroannelated methanofullerenes bearing quinone-type addends including TCNQ and DCNQI analogues (**3a**−**c**, **6a,b**, **8**, **10,** and **11**) have been prepared, and their structural and electronic properties have been characterized by both experimental techniques and quantum-chemical calculations. The spiro[2,5-cyclohexadienone-4,61′-methanofullerene] derivatives (**3a**−**c**), the spiro[10-anthrone-9,61′-methanofullerene] (**8**), and the TCNQ- and DCNQI-type derivatives (**10** and **11**) were isolated as [6,6] adducts. The spiro[cyclohexanone-4,61′-methanofullerene] (**6**) was however obtained as a mixture of [5,6] and [6,6] isomers. The novel methanofullerenes, with the only exception of **6**, show irreversible cyclic voltammograms with additional reduction peaks. The conjugated cyclohexadienone derivatives **3** exhibit better acceptor abilities than the parent C_{60}. Semiempirical PM3 calculations show that the addend lies perpendicular to the transanular bond in **3**, while it folds down and adopts a butterfly shaped structure for compounds **8**, **10,** and **11.** For compounds **3**, periconjugative interactions transmit the inductive effect of the addend and produce a small stabilization of the orbitals of C_{60}, resulting in a less negative first-reduction potentials compared to C_{60}. For compounds **8**, **10,** and **11,** the folding of the addend prevents periconjugative effects. Theoretical calculations performed on $\mathbf{3a}^{\bullet-}$ and $\mathbf{3a}^{2-}$ at the semiempirical (PM3), density functional (B3P86/3-21G), and ab initio (HF/6-31G*) levels indicate that the attachment of the first electron causes the homolytic cleavage of one of the bonds connecting the addend to C_{60}. The resulting open-cyclopropane structure is stabilized by the aromaticity of the phenoxyl radical structure presented by the addend. The second electron enters in the addend forming the phenoxyl anion. This ring opening is supported by ESR measurements and explains the irreversible electrochemical behavior of compounds **3**. The nonconjugated nature of the cyclohexanone ring in **6** determines that reduction takes place via a closed-cyclopropane structure with an electrochemical behavior similar to that observed for C_{60}. Compounds **8**, **10,** and **11** are proposed to undergo reduction via an open-cyclopropane structure now obtained after the attachment of the second electron which produces the heterolytic opening of the cyclopropane ring. The lack of planarity shifts the reduction of the addend to more negative potentials.

Introduction

The design of novel organofullerenes exhibiting better electron acceptor properties than the parent fullerene C_{60} is a major goal for the development of specific electronic and optical applications.[1] The charge-transfer absorption energies measured for different donor−C_{60} complexes in solution, together with the redox potentials and the electron affinity reported for the fullerene C_{60} molecule, clearly indicate that C_{60} is a weak electron acceptor comparable to other organic molecules such as *s*-tetracyanobenzene or 2,3-dichloro-1,4-naphthoquinone.[2,3]

In agreement with the observed electron-accepting ability, complexation reactions of C_{60} with strong electron donors such as cobaltocene[4] or tetrakis(dimethylamino)ethylene (TDAE)[5] have been reported to form fully ionic charge-transfer complexes (CTC). The $[TDAE^+]C_{60}^-$ complex thus shows low room-temperature conductivity but exhibits interesting ferromagnetic properties.[6] Clathration with other donor organic molecules such as ferrocene,[7] bis(ethylenedithio)tetrathiafulvalene (BEDT-TTF),[8] its dimer,[9] $Fe(CO)_4(\eta^5\text{-}C_5H_5)_4$,[10] hexamethylenetetratel-

[†] University of California.
[‡] Universidad Complutense.
[§] Universidad de Valencia.
[||] CSIC.
[⊗] Abstract published in *Advance ACS Abstracts,* August 15, 1997.

(1) Hirsch, A. *The Chemistry of the Fullerenes*; Thieme: New York, 1994.
(2) Saito, G.; Teramoto, T.; Otsuka, A.; Sugita, Y.; Ban, T.; Kusunoki, M.; Sakaguchi, K. *Synth. Met.* **1994**, *64*, 359.
(3) Wang, L. S.; Conceiao, J.; Jin, C.; Smalley, R. E. *Chem. Phys. Lett.* **1991**, *182*, 5.
(4) Stinchcombe, J.; Penicaud, A.; Bhyrappa, P.; Boyd, P. D. W.; Reed, C. A. *J. Am. Chem. Soc.* **1993**, *115*, 5212.
(5) Stephens, P. W.; Cox, D.; Lauher, J. W.; Mihaly, L.; Wiley: J. B.; Allemand, P.-M.; Hirsch, A.; Holczer, K.; Li, Q.; Thompson, J. D.; Wudl, F. *Nature* **1992**, *355*, 331.
(6) Allemand, P.-M.; Khemani, K. C.; Koch, A.; Wudl, F.; Holczer, K.; Donovan, S.; Grüner, G.; Thompson, J. D. *Science* **1991**, *253*, 301.
(7) Crane, J. D.; Hitchcock, P. B.; Kroto, H. W.; Taylor, R.; Walton, D. R. M. *J. Chem. Soc., Chem. Commun.* **1992**, 1764.
(8) Izuoka, A.; Tachikawa, T.; Sugawara, T.; Suzuki, Y.; Konno, M.; Saito, Y.; Shinohara, H. *J. Chem. Soc., Chem. Commun.* **1992**, 1472.

S0002-7863(96)02299-8 CCC: $14.00

lurafulvalene (HMTTeF),[11] or the more recent tellurium donor derivatives[12] results in the formation of insulating neutral solids in which the C_{60} molecule cocrystallizes with the donor unit. Intramolecular charge-transfer electronic interactions between C_{60} and a series of electron donor moieties have also been recently reported.[13]

The preparation of electrically conducting CT complexes containing the C_{60} unit requires the design of electroactive organofullerenes showing improved electrochemical properties in comparison with the parent C_{60} molecule. In this regard, although a wide variety of C_{60} derivatives bearing different addends have been prepared,[14] their electrochemical properties have been scarcely reported, and only recently, a comparative electrochemical study by cyclic voltammetry of a group of differently modified organofullerenes has been published by Suzuki et al.[15] The electrochemical behavior of a series of organofullerenes has also been analyzed beyond the fourth-reduction wave by Echegoyen et al.[16] With the exception of the highly fluorinated $C_{60}F_{48}$[17] and the recently reported dicyanodihydrofullerene,[18] which show more positive first-reduction potentials, the fullerene derivatives studied by Suzuki et al.[15] show cathodically shifted potentials relative to C_{60} due to the saturation of a double bond in the sphere. Suzuki et al. concluded that the inductive effect of the attached organic group was the most important factor in determining the redox properties of organofullerenes.[15]

The first-reduction potentials of the spiroannelated fluorenofullerenes (**1**) shown in Figure 1 have been recently reported to be dependent on the electronic nature of the substituent R.[19] For compounds bearing electron-donating groups (**1b**), the first- and second-reduction potentials are shifted to more negative values relative to unsubstituted C_{60}, while for compounds bearing electron-withdrawing groups (**1c**), both potentials show slightly less negative values than for C_{60}. This behavior contrasts with that observed for diphenylmethanofullerenes, for which the CV data are independent of the functional groups. The existence of a special kind of through-space orbital interactions between the π-systems of the ball and the spiroannelated addend in **1** was invoked as the crucial difference with diphenylmethanofullerenes. The so-called "periconjugation" [20] can be thus considered as an alternative and predictable procedure for the preparation of novel spiroannelated methanofullerenes exhibiting anodically shifted peaks, relative to C_{60}, as precursors for the preparation of molecular materials with electrical, optical, and magnetic properties.

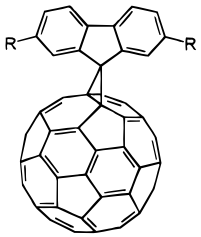

1a : R = H
1b : R = NBn_2
1c : R = NO_2

Figure 1. Fluorenofullerenes with electron-donating and electron-withdrawing substituents.

In this paper, we describe the synthesis of a series of prototype quinone-type methanofullerenes (**3**, **6**, and **8**). The effect of substitution on the electrochemical properties is studied for compound **3**. Furthermore, we have carried out the additional transformation of compound **8** to the corresponding dicyanomethylene and cyanoimino derivatives (**10** and **11**) as intended analogues of tetracyano-*p*-quinodimethane (TCNQ) and dicyano-*p*-quinonediimine (DCNQI). We combine cyclic voltammetry and spectroscopic measurements with quantum-chemical calculations to characterize the compounds prepared and to gain some understanding of the experimentally observed trends.

Results and Discussion

Synthesis. The quinone-type methanofullerenes were prepared by following the versatile fullerene functionalization by reaction of organic diazo compounds with C_{60}.[21] In a preliminary communication, we reported the reaction of C_{60} with the corresponding 1,4-diazooxides to afford the novel carbonyl-containing organofullerenes[22] (Scheme 1). 1,4-Diazooxides were in turn prepared according to the procedures previously reported in the literature.[23,24]

The spiro[2,5-cyclohexadienone-4,61′-methanofullerene] derivatives **3a**−**c** were isolated exclusively as adducts on 6/6 junctions according to spectroscopic data.[22] A different behavior was observed in the photochemical reaction of the carbonyl protected tosylhydrazone **4** with C_{60}, leading to a mixture of fulleroid (**5a**) and methanofullerene (**5b**) isomers, from which the free carbonyl [5,6]- and [6,6]-spiro[cyclohexanone-4,61′-methanofullerenes] **6a**,**b** could be separated and characterized

(9) Izuoka, A.; Tachikawa, T.; Sugawara, T.; Saito, Y.; Shinohara, H. *Chem. Lett*. **1992**, 1049.
(10) Crane, J. D.; Hitchcock, P. B. *J. Chem. Soc., Dalton Trans*. **1993**, 2537.
(11) Pradeep, T.; Singh, K. K.; Sinha, A. P. B.; Morris, D. E. *J. Chem. Soc., Chem. Commun*. **1992**, 1747.
(12) Wang, P.; Lee, W.-J.; Shcherbakova, I.; Cava, M. P.; Metzger, R. M. *Synth. Met.* **1995**, *70*, 1457.
(13) Liddell, P. A.; Kuciauskas, D.; Sumida, J. P.; Nash, B.; Nguyen, D.; Moore, A. L.; Moore, T. A.; Gust, D. *J. Am. Chem. Soc.* **1997**, *119*, 1400. Guldi, D. M.; Maggini, M.; Scorrano, G.; Prato, M. *J. Am. Chem. Soc*. **1997**, *119*, 974. Kuciauskas, D.; Lin, S.; Seely, G. R.; Moore, A. L.; Moore, T. A.; Gust, D.; Drovetskaya, T.; Reed, Ch. A.; Boyd, P. D. W. *J. Phys. Chem*. **1996**, *100*, 15926. Imahori, H.; Hagiwara, K.; Aoki, M.; Akiyama, T.; Taniguchi, S.; Okada, T.; Shirakawa, M.; Sakata, Y. *J. Am. Chem. Soc*. **1996**, *118*, 11771. Williams, R. M.; Koeberg, M.; Lawson, J. M.; An, Y.-Z.; Rubin, Y.; Paddon-Row, M. N.; Verhoeven, J. W. *J. Org. Chem*. **1996**, *61*, 5055. Matsubara, Y.; Tada, H.; Nagase, S.; Yoshida, Z. *J. Org. Chem*. **1995**, *60*, 5372. Williams, R. M.; Zwier, J. M.; Verhoeven, J. W. *J. Am. Chem. Soc*. **1995**, *117*, 4093. Nakamura, Y.; Minowa, T.; Tobita, S.; Shizuka, H.; Nishimura, J. *J. Chem. Soc., Perkin Trans 2*, **1995**, 2351. Imahori, H.; Hagiwara, K.; Akiyama, T.; Taniguchi, S.; Okada, T.; Sakata, Y. *Chem. Lett*., **1995**, 265. Watanabe, A.; Ito, O. *J. Chem. Soc., Chem. Commun*. **1994**, 1285. Belik, P.; Gügel, A.; Kraus, A.; Spikermann, J.; Enkelmann, V.; Frank, G.; Müllen, K. *Adv. Mater*. **1993**, *5*, 854. Diederich, F.; Jonas, U.; Gramlich, U.; Hermann, A.; Ringsdorf, H.; Thilgen, C. *Helv. Chim. Acta* **1993**, *76*, 2445. Khan, S. J.; Oliver, A. M.; Paddon-Row: M. N.; Rubin, Y. *J. Am. Chem. Soc*. **1993**, *115*, 4919.
(14) Diederich, F.; Thilgen, C. *Science* **1996**, *271*, 317. Hirsch, A. *Synthesis* **1995**, 895.
(15) Suzuki, T.; Maruyama, Y.; Akasaka, T.; Ando, W.; Kobayashi, K.; Nagase, S. *J. Am. Chem. Soc*. **1994**, *116*, 1359.
(16) Arias, F.; Xie, Q.; Wu, Y.; Lu, Q.; Wilson, S. R.; Echegoyen, L. *J. Am. Chem. Soc*. **1994**, *116*, 6388.
(17) Zhou, F.; Van Berkel, G. J.; Donovan, B. T. *J. Am. Chem. Soc*. **1994**, *116*, 5485.
(18) Keshavarz-K., M.; Knight, B.; Srdanov, G.; Wudl, F. *J. Am. Chem. Soc*. **1995**, *117*, 11371.
(19) Eiermann, M.; Haddon, R. C.; Knight, B.; Chan Li, Q.; Maggini, M.; Martín, N.; Ohno, T.; Prato, M.; Suzuki, T.; Wudl, F. *Angew. Chem., Int. Ed. Engl*. **1995**, *34*, 1591.
(20) Wudl, F.; Suzuki, T.; Prato, M. *Synth. Met*. **1993**, *59*, 297.
(21) Suzuki, T.; Li, Q.; Khemani, K. C.; Wudl, F.; Almarsson, Ö. *Science* **1991**, *254*, 1186. Shi, S.; Khemani, K. C.; Li, Q.; Wudl, F. *J. Am. Chem. Soc*. **1992**, *114*, 10656. Suzuki, T.; Li, Q.; Khemani, K. C.; Wudl, F. *J. Am. Chem. Soc*. **1992**, *114*, 7300. Prato, M.; Suzuki, T.; Wudl, F. *J. Am. Chem. Soc*. **1993**, *115*, 7876. Prato, M.; Lucchini, V.; Maggini, M.; Stimpfl, E.; Scorrano, G.; Eiermann, M.; Suzuki, T.; Wudl, F. *J. Am. Chem. Soc*. **1993**, *115*, 8479.
(22) Ohno, T.; Martín, N.; Knight, B.; Wudl, F.; Suzuki, T.; Yu, H. *J. Org. Chem*. **1996**, *61*, 1306.
(23) Puza, M.; Doetschman, D. *Synthesis* **1971**, 481.
(24) Ried, W.; Dietrich, R. *Chem. Ber*. **1961**, *94*, 387.

Scheme 1

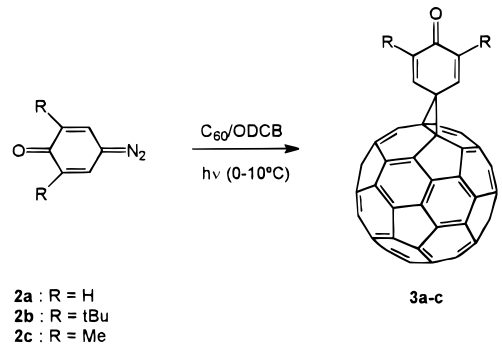

Scheme 2

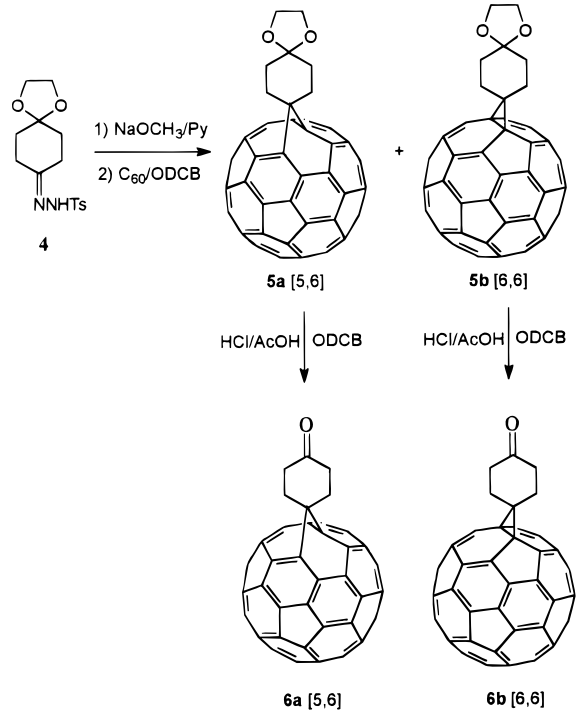

(Scheme 2). In this case, the diazo compound was generated in situ from tosylhydrazone **4** by base treatment, followed by reaction with C_{60} under standard conditions. It has been previously observed that fulleroids are the kinetic products of these diazo additions to C_{60}.[25] Fulleroids can, in general, be transformed by thermalization into the thermodynamically more stable methanofullerenes.[26] More recent, photochemical isomerization has also been reported.[27] Thus, the isomeric mixture **5a,b** either under thermal or photochemical conditions afforded the methanofullerene (**5b**). As it is shown in Scheme 2, further treatment of the isolated isomers under acidic conditions yielded the cyclohexanone derivatives **6a** and **6b,** respectively.

In contrast to the monocyclic 1,4-diazooxides **2a**−**c**, 10-diazoanthrone (**7**) reacted smoothly with C_{60} under different thermal conditions (see Table S1 in the Supporting Information). Together with the monoadduct spiro[10-anthrone-9,61′-methanofullerene] (**8**) obtained in moderate yield,[22] a mixture of isomeric bis adducts (**9**, $n = 2$) and tris adducts (**9**, $n = 3$) were obtained.

Quinone-type spiromethanofullerenes are good candidates for the preparation of TCNQ-type and DCNQI-type derivatives. TCNQ and DCNQI are among the most useful electron-acceptor molecules for the preparation of salts and charge-transfer complexes exhibiting electrically conducting behavior.[28] π-Extended acceptor systems based on TCNQ and DCNQI have been recently reported to present interesting photoinduced intramolecular electron-transfer properties.[29,30] The linkage of TCNQ- or DCNQI-type acceptor units to C_{60} showing through-space orbital interactions should lead to the preparation of novel and stronger C_{60} containing acceptors.

We have carried out the reaction of the spiromethanofullerene **8** with malononitrile in the presence of a large excess of titanium tetrachloride and pyridine (Lehnert's reagent).[31] The reaction, that is performed in refluxing dry chloroform, proceeds slowly (7−14 days) in moderate yield (26%; 37% based on consumed C_{60}) (Scheme 3). The UV−vis spectrum of the dicyanomethylene derivative **10** shows the characteristic peaks for the methanofullerene isomers at 434, 492, and 694 nm, and the FTIR presents the conjugated cyano band at 2223 cm^{-1}. The methanofullerene structure had already been previously ascertained for the quinone-type precursor (**8**) by ^{13}C NMR spectroscopy.[22]

The preparation of the DCNQI-type methanofullerene **11** was obtained from **8** by reaction with bis(trimethylsilyl)carbodiimide (BTC) and titanium tetrachloride by following Hünig's procedure[32] (Scheme 3). Analogously to the preparation of **10**, the reaction of **8** and BTC takes place slowly in refluxing dry chloroform and requires a large excess of reactants, affording the cyanoimino methanofullerene (**11**) in good yield (60% and the starting compound **8** was consumed). The comparatively long reaction times needed for the preparation of compounds **10** and **11** indicate the lower reactivity of this carbonyl group in comparison with other π-extended quinones.[33] This fact could be accounted for by the proximity of the surface of the ball to the carbonyl group. This effect has been previously observed for other functional groups (ester) close to the sphere.[34]

Compound **11** shows the expected UV−vis peaks at 435, 498, and 698 nm and the cyano stretching vibration at 2171 cm^{-1}. FAB-MS shows the MH^+ ion for compound **11** at 937 (calcd for $C_{75}H_8N_2$, 937.0766; found, 937.0762) and, analogously, at 961 for compound **10**, being the base peak at 720 (C_{60}). The ^1H NMR (CS_2/500 MHz) spectrum of **10** shows the aromatic *peri* hydrogens as two multiplets at $\delta = 8.28$ and 8.08, integrating each one for two protons. For compound **11**, four doublets appear at $\delta = 8.65$ (1H), 8.40 (1H), 8.33 (1H), and 8.10 (1H), thus indicating the loss of symmetry for the cyanoimino derivative.

(25) Suzuki, T.; Li, Q.; Khemani, K. C.; Wudl, F. *J. Am. Chem. Soc.* **1992**, *114*, 7301. Isaacs, L.; Wehrsig, A.; Diederich, F. *Helv. Chim. Acta* **1993**, *76*, 1231.

(26) Smith, A. B., III; Strongin, R. M.; Brard, L.; Furst, G. T.; Romanow, W. J.; Owens, K. G.; King, R. C. *J. Am. Chem. Soc.* **1993**, *115*, 5829. Osterodt, J.; Nieger, M.; Windschief, P.-M.; Vögtle, F. *Chem. Ber.* **1993**, *126*, 2331.

(27) González, R.; Hummelen, J. C.; Wudl, F. *J. Org. Chem.* **1995**, *60*, 2618.

(28) International Conference on Science and Technology of Synthetic Metals, ICSM94, Seoul, Korea. See also: Martín, N.; Seoane, C. In *Organic Conductive Molecules and Polymers*; Nalwa, N. S., Ed.; Wiley: New York, 1997. *New Organic Materials*; Seoane, C., Martín, N., Eds; Universidad Complutense, 1994.

(29) Martín, N.; Segura, J. L.; Seoane, C.; De la Cruz, P.; Langa, F.; Ortí, E.; Viruela, P. M.; Viruela, R. *J. Org. Chem.* **1995**, *60*, 4077.

(30) Martín, N.; Segura, J. L.; Seoane, C.; Ortí, E.; Viruela, P. M.; Viruela, R.; Albert, A.; Cano, F. H.; Vidal, J.; Rovira, C.; Veciana, J. *J. Org. Chem.* **1996**, *61*, 3041.

(31) Lehnert, W. *Tetrahedron Lett.* **1970**, 4723; Lehnert, W. *Synthesis* **1974**, 667.

(32) Aumüller, A.; Hünig, S. *Angew. Chem., Int. Ed. Engl.* **1984**, *23*, 447. Hünig, S.; Erk, P. *Adv. Mater.* **1991**, *3*, 225.

(33) Martín, N.; Behnisch, R.; Hanack, M. *J. Org. Chem.* **1989**, *54*, 2563.

(34) Win, W. W.; Kao, M.; Eiermann, M.; McNamara, J. J.; Wudl, F.; Pole, D. L.; Kassam, K.; Warkentin, J. *J. Org. Chem.* **1994**, *59*, 5871; Meier, M. S.; Poplawska, M. *Tetrahedron* **1996**, *52*, 5043.

Scheme 3

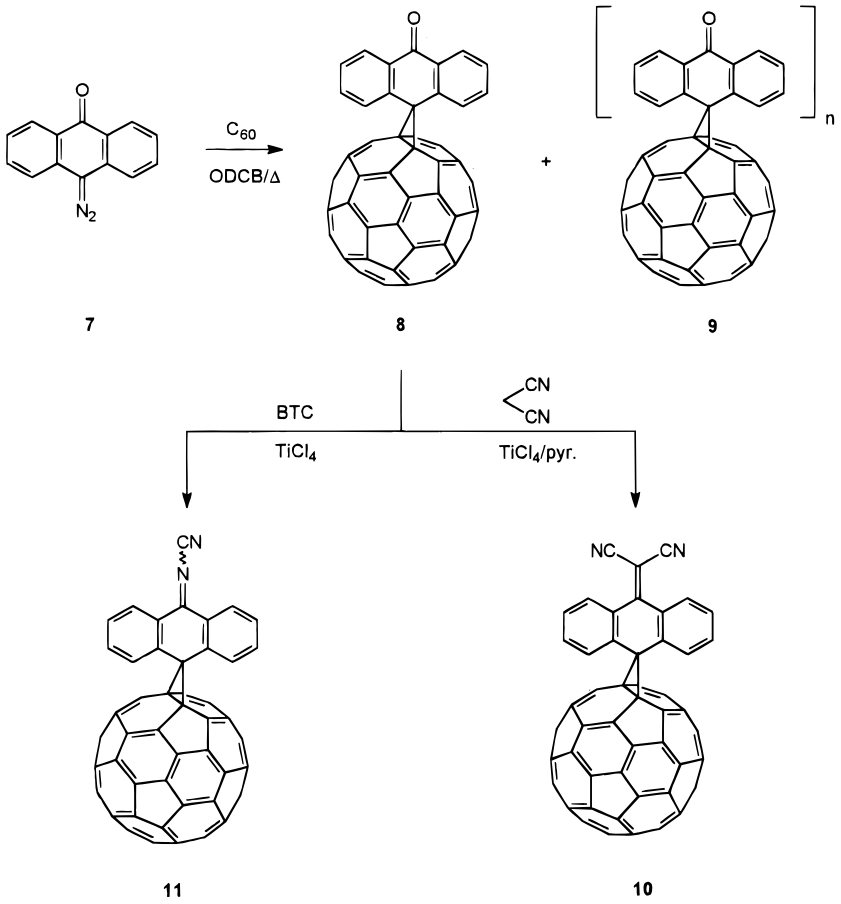

Attempts to carry out the reaction of the monocyclic quinone-type methanofullerenes **3a**−**c** with malononitrile or BTC under the same experimental conditions did not lead to the respective dicyanomethylene or cyanoimino derivatives. The low solubility of compound **3a** and the steric hindrance of the substituents adjacent to the low reactive carbonyl group in **3b**,**c** prevented the progress of the reaction.

Electrochemistry. The cyclic voltammetry (CV) measurements were carried out in 1,2-dichlorobenzene (ODCB) at room temperature with tetrabutylammonium tetrafluoroborate as the supporting electrolyte.[35] Peak reduction potentials instead of averaged data are summarized in Table 1 since several irreversible processes were observed. Figure 2 displays the cyclic voltammograms obtained for **3c**, **6b**, and **10**.

The CV curves recorded for the fulleroid **6a** and the methanofullerene **6b** indicate that the first reduction of both isomers is totally reversible and occurs at slightly more negative values in comparison with the unsubstituted C_{60}, in agreement with the expected behavior for organofullerenes.[15] Isomers 5/6 and 6/6 are reported to present a similar electrochemical behavior for the first four reduction waves, and only recently, an anodically shifted (0.20 V) fifth-reduction wave has been observed for a fulleroid, in comparison with that of the corresponding methanofullerene.[36] In this regard, the CV data of the fulleroid form **6a** closely correspond to those measured for the methanofullerene form **6b**, especially for the first- and second-reduction waves. The four-reduction waves observed for both isomers clearly correlate with those measured for C_{60}.

Table 1. Peak Reduction Potentials (mV vs Ferrocene/Ferrocenium)

compd	E^1_{red}	E^2_{red}	E^3_{red}	E^4_{red}	E^5_{red}
C_{60}	−1123	−1455	−1913	−2383	
3a	−1081[a,c]	−1559[c]			
3b	−1097[b]	−1620	−2037		
3c	−1042	−1197	−1602	−2016	
6a	−1158	−1550	−2010	−2379	
6b	−1164	−1554	−2044	−2504	
8	−1215	−1525	−1670	−2090	
10	−1133	−1383	−1537	−1943	
11	−1142	−1321	−1448	−1536	−1953

[a] Peak position depends on scan rate. [b] Two-electron process. [c] Scan rate: 10 mV s^{-1}.

In comparison with isomers **6a**,**b**, the quinone-type derivatives **3a**−**c** show a significantly different electrochemical behavior. On one hand, the first-reduction potential of **3a**−**c** is anodically shifted with respect to C_{60}. This result evidence the striking influence of the double bonds present in the cyclohexadienone addend. Derivatives that undergo reduction more easily than unsubstituted C_{60} are still rare, and the quest for more electronegative spiroannelated methanofullerenes can enhance the outstanding properties of the C_{60} molecule. On the other hand, and unlike most organofullerenes, compounds **3a**−**c** show an irreversible behavior in the CV measurements. This fact could be accounted for by the opening of the cyclopropane ring in the formation of the radical anion[19] and is discussed below in the light of theoretical calculations and ESR measurements. It should be also mentioned that the first-reduction wave of **3b** corresponds to a two-electron process and for **3c** presents a

(35) CV conditions: 0.15 M (^{n}Bu)$_4$NBF$_4$ in *o*-dichlorobenzene, 25 °C. Working electrode: Pt disk (2 mm diameter). Counter electrode: Pt wire. Reference electrode: aqueous Ag/AgCl (Fc/Fc$^+$ internal standard). Potentiostat: BAS-100A, scan rate 100 mV s^{-1}. Other standard CV solvents (THF, acetonitrile) as well as toluene/acetonitrile (Xie, Q.; Pérez-Cordero, E.; Echegoyen, L. *J. Am. Chem. Soc.* **1992**, *114*, 3978) did not provide sufficient solubility for all compounds of our study.

(36) Arias, F.; Echegoyen, L.; Wilson, S. R.; Lu, Q. *J. Am. Chem. Soc.* **1995**, *117*, 1422.

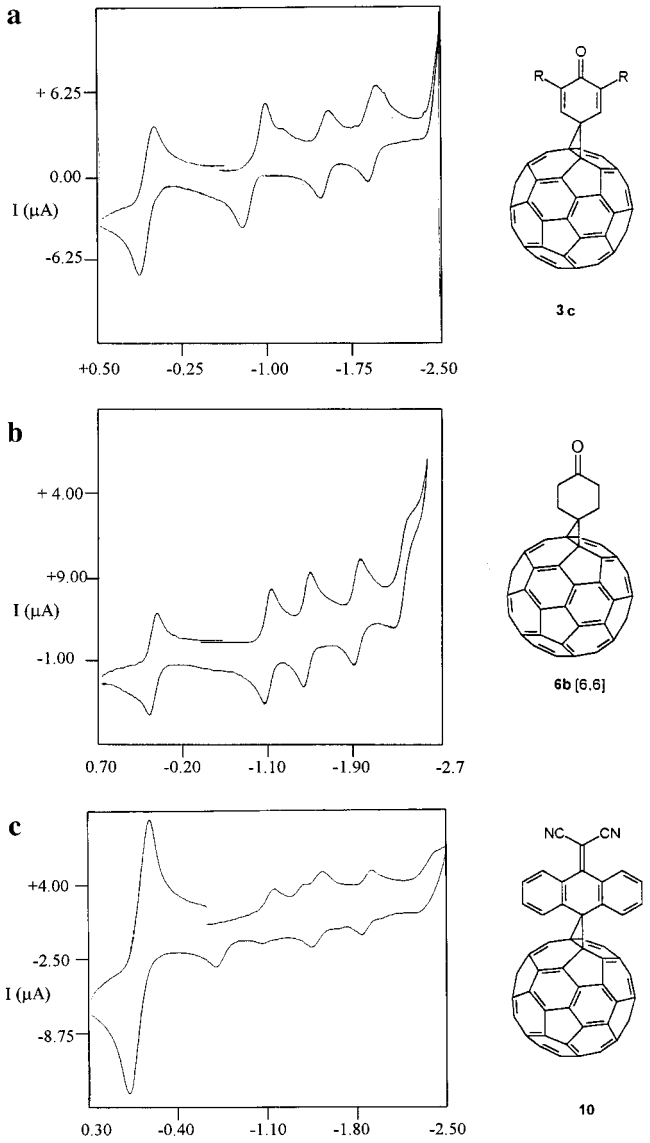

Figure 2. Cyclic voltammograms of compounds **3c**, **6b**, and **10**. Scan rate: 100 mV s^{-1}. Potentials vs ferrocene/ferrocenium (Fc/Fc^+).

shoulder at −1197 mV. The poor quality of the CV data recorded for unsubstituted **3a** is due to the extremely low solubility of this compound.

The anthrone-containing methanofullerene **8** shows a first-reduction potential shifted toward more negative values than those for compounds **3a**−**c** and C_{60}. The Osteryoung square wave voltammetry (OSWV)[37] was also recorded and confirms the obtained CV values. Preliminary molecular mechanics calculations showed that the steric interactions of the *peri* hydrogens of the anthrone moiety with the surface of the fullerene causes the deviation of the orthogonal disposition of the addend.[22] The effect of this geometric distortion on the electronic properties is discussed below.

The CV data recorded for the dicyanomethylene **10** and cyanoimino **11** derivatives show that their first reductions are irreversible and occur at −1133 and −1142 mV, respectively (see Figure 2c and Table 1). In comparison with the precursor anthrone-containing spiromethanofullerene **8**, the reduction is facilitated by more than 70 mV (Table 1), thus showing the stronger electronic effect of the dicyanomethylene and cyanoimino groups.[38] Compounds **10** and **11** present several reduction processes in the voltage zone −1300 to −1600 mV.

(37) Osteryoung, J. G.; O'dea, J. J. In *Electroanalytical Chemistry*; Bard, A. J., Ed.; Dekker: New York, 1986; Vol. 14.

Although synthetic difficulties prevented the preparation of the respective TCNQ and DCNQI-type methanofullerenes of the quinone-type **3a**−**c,** the less negative reduction potentials obtained for **10** and **11** compared to **8** suggest that those methanofullerenes would present anodically shifted reduction potentials related to compounds **3a**−**c**. The design of novel quinone-type methanofullerenes bearing long alkyl chains, to increase their solubility, or with fused pentagonal heterocyclic rings are currently under investigation in our groups.

Theoretical Calculations. To gain some understanding of the experimental observations reported above, quantum-chemical calculations were performed for compounds **3a**, **6b**, **8**, **10**, and **11**. The molecular geometries were fully optimized using the PM3 semiempirical method[39] as implemented in the MOPAC 93[40] and GAUSSIAN 94[41] systems of programs. The geometries of the unsubstituted methanofullerene $C_{60}CH_2$, cyclopentadienefullerene ($C_{60}C_5H_4$), and fluorenofullerene ($C_{60}C_{13}H_8$) were optimized for comparison purposes. Additional calculations at the ab initio Hartree−Fock (HF) level and using density functional theory (DFT) were performed for **3a**. DFT calculations have the advantage of providing electron-correlated wave functions at a reasonable computer cost and are being extensively applied to the study of fullerenes.[42−44]

Molecular Structure. Figure 3 presents the PM3-optimized geometry obtained for **3a** without imposing any symmetry restriction. The quinone ring perpendicularly bisects the C1−C2 bond and forms a methanofullerene structure with the fullerene cage. Compound **3a** thus shows a C_{2v} symmetry in accord with the 15 peaks observed for the fullerene moiety in the ^{13}C NMR spectrum indicating the existence of two planes of symmetry.[22] Figure 3 only displays the bond lengths and bond angles of the pyracylene unit defined around the 6/6 junction where bridging occurs because the geometry of this unit undergoes the most noticeable changes with respect to C_{60}. For C_{60}, the PM3 method predicts bonds lengths of 1.458 and 1.384 Å for 5/6 and 6/6 junctions, respectively, in good agreement with the experimental values obtained from X-ray data (1.446 and 1.389 Å)[45] and gas-phase electron diffraction measurements (1.458 and 1.401 Å).[46]

The methano-bridged C1−C2 bond is predicted to have a length of 1.548 Å, i.e., 0.164 Å longer than the 6/6 junctions in C_{60}. The calculated value is slightly shorter than the experimental X-ray bond distances reported for (bis((trimethylsilyl)-butadiynyl)methano)fullerene (1.574 Å)[47] and ((3,4-dimethox-

(38) Hünig, S. *Pure Appl. Chem.* **1990**, *62*, 395.
(39) Stewart, J. J. P. *J. Comput. Chem.* **1989**, *10*, 209, 221.
(40) MOPAC 93: J. J. P. Stewart, Fujitsu Limited, Tokyo, Japan, 1993
(41) Frisch, M. J.; Trucks, G. W.; Schlegel, H. B.; Gil, P. M. W.; Johnson, B. G.; Robb, M. A.; Cheeseman, J. R.; Keith, T.; Petersson, G. A.; Montgomery, J. A.; Raghavachari, K.; Al-Laham, M. A.; Zakrzewski, V. G.; Ortiz, J. V.; Foresman, J. B.; Cioslowski, J.; Stefanov, B. B.; Nanayakkara, A.; Challacombe, M.; Peng, C. Y.; Ayala, P. Y.; Chen, W.; Wong, M. W.; Andres, J. L.; Replogle, E. S.; Gomperts, R.; Martin, R. L.; Fox, D. J.; Binkley, J. S.; Defrees, D. J.; Baker, J.; Stewart, J. P.; Head-Gordon, M.; Gonzalez, C.; Pople, J. A. *Gaussian 94, Revision B.1*; Gaussian Inc.: Pittsburgh, PA, 1995.
(42) Martin, J. M. L.; El-Yazal, J.; François, J.-P. *Chem. Phys. Lett.* **1995**, *242*, 570; **1996**, *52*, 9. Martin, J. M. L. *Chem. Phys. Lett.* **1996**, *255*, 1.
(43) (a) Raghavachari, K.; Sosa, C. *Chem. Phys. Lett.* **1993**, *209*, 223. (b) Bakowies, D.; Bühl, M.; Thiel, W. *Chem. Phys. Lett.* **1995**, *247*, 491. (c) Scuseria, G. E. *Chem. Phys. Lett.* **1996**, *257*, 583. (d) Patchkovskii, S.; Thiel, W. *J. Am. Chem. Soc.* **1996**, *118*, 7164.
(44) Green, W. H. Jr.; Gorun, S. M.; Fitzgerald, G.; Fowler, P. W.; Ceulemans, A.; Titeca, B. C. *J. Phys. Chem.* **1996**, *100*, 14892.
(45) Bürgi, H.-B.; Blanc, E.; Schwarzenbach, D.; Liu, S.; Lu, V.; Kappes, M. M.; Ibers, J. A. *Angew. Chem., Int. Ed. Engl.* **1992**, *31*, 640.
(46) Hedberg, K.; Hedberg, L.; Bethune, D. S.; Brown, C. A.; Dorn, H. C.; Johnson, R. D.; de Vries, M. *Science* **1991**, *254*, 410.
(47) Anderson, H. L.; Boudon, C.; Diederich, F.; Gisselbrecht, J.-P.; Gross, M.; Seiler, P. *Angew. Chem., Int. Ed. Engl.* **1994**, *33*, 1628.

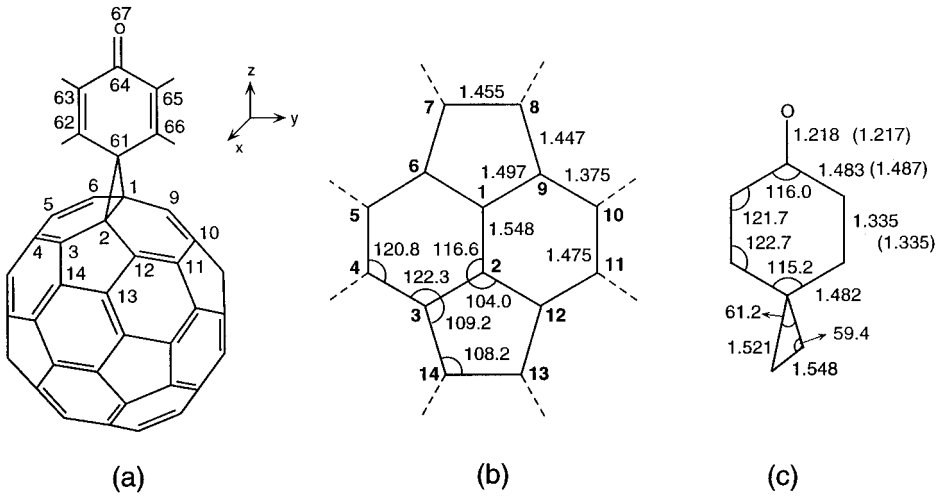

Figure 3. Detail of the PM3-optimized molecular structure of compound **3a**. (a) Atom numbering and axes orientation. (b) Geometry of the pyracylene unit on which methano bridging takes place. (c) Geometry of the cyclohexadienone moiety. The PM3-optimized bond lengths obtained for *p*-benzoquinone are given within parentheses. Bond lengths are in angstroms and bond angles in degrees.

yphenyl)methano)fullerene (1.614 Å),[48] and is in good agreement with the X-ray value of 1.553 Å reported for a methano-bridged dibenzohomopyracylene.[47,49] The lengthening of the C1−C2 bond is accompanied by the elongation of the four contiguous 5/6 bonds (1.497 Å) which have sp^3-sp^2 character. The remaining bonds forming the pyracylene unit depicted in Figure 3b present maximum deviations of 0.017 and 0.009 Å with respect to the bond distances of the 5/6 and 6/6 bonds in C_{60}, respectively.

The bond angles surrounding the transannular C1−C2 bond present the largest deviations from the values of 120 and 108° found for the internal angles of hexagons and pentagons, respectively, in icosahedral C_{60}. The C6−C1−C9 and C3−C2−C12 angles are reduced to 104.0° and the C6,C9−C1−C2 and C3,C12−C2−C1 angles to 116.6° in agreement with the 106.0 and 116.2° values reported for (bis((trimethylsilyl)-butadiynyl)methano)fullerene.[47]

The strain at the bridgehead atoms C1 and C2 determines that the two hexagons and the two pentagons delimiting the C1 and C2 vertices lose their planarity and fold up. The hexagons present a folding angle of 6.4° along the C3−C6 and C9−C12 axes, respectively. The pentagons are more largely bent along the C3−C12 and C6−C9 axes by angles of 10.5°. As a consequence of these foldings, the C1 and C2 atoms protrude from the C_{60} skeleton. The distances from these two atoms to the centroid of the ball are 3.765 Å and are larger than the distances from the atoms situated on the opposite pole of C_{60} (3.541 Å) or from the atoms located on the equatorial zone along the *y* (3.530 Å) and *x* (3.551 Å) axes. All these trends agree with those observed by Anderson et al. from X-ray experimental data.[47]

The cyclohexadienone ring is joined to the C1 and C2 atoms by bonds of 1.521 Å. This value lies between the average values reported for a (diphenylmethano)fullerene (1.512 Å)[48] and for (bis((trimethylsilyl)butadiynyl)methano)fullerene (1.539 Å).[47] The C1−C61−C2 angle predicted for **3a** (61.2°) is very close to that obtained for the latter (61.6°).[47] The geometry of the cyclohexadienone moiety is typical of a quinone-type structure with a large bond length alternancy between single and double bonds (see Figure 3c).

The PM3-optimized geometries calculated for the methano-fullerene moiety in compounds **6b**, **8**, **10**, **11,** $C_{60}CH_2$, and $C_{60}C_5H_4$ are almost identical with that obtained for **3a** and show the same trends. (The geometric parameters defining the cyclopropane ring in these compounds are given in Table S2 as Supporting Information). **3a** presents the narrowest cyclopropane ring due to the nonbonding interactions that take place between the two lower hydrogen atoms (H62 and H66) of the cyclohexadienone moiety and the C3 to C6 and C9 to C12 atoms of the C_{60} ball. The distances for these interactions are 2.71 and 2.79 Å, which are slightly shorter than the sum of the van der Waals radii for carbon and hydrogen (2.90 Å).[50]

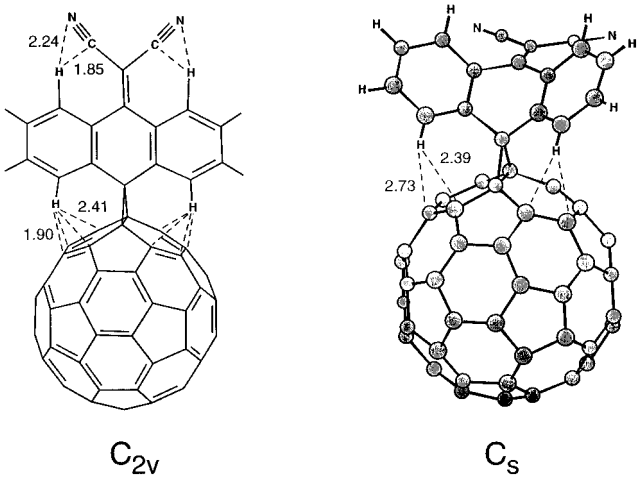

Figure 4. PM3-optimized C_{2v} and C_s structures of compound **10**. See Figure 3 for atom numbering.

Steric interactions are more important for the anthracenofullerenes **8**, **10**, and **11** due to the short contacts between the aromatic *peri* hydrogens of the anthracene unit and the C_{60} ball. As depicted in Figure 4, the PM3-optimized geometry calculated for **10** imposing a C_{2v} symmetry reveals that the distance of the *peri* hydrogens to the C4, C5 and C10, C11 atoms is only 1.90 Å and the distance to the C3, C6 and C9, C12 atoms is 2.41 Å. To avoid these short contacts, the anthracene moiety is no longer perpendicular to the C1−C2 bond and its central ring is folded adopting a boat conformation. The resulting C_s structure only shows two short contacts at 2.39 Å between the two lower *peri* hydrogens and carbons C3 and C12. Similar structures are found for **8** and **11**.

For compound **8**, the folded C_s structure is 25.18 kcal/mol more stable than the perpendicular C_{2v} form. The "butterfly

(48) Osterodt, J.; Nieger, M.; Vögtle, F. *J. Chem. Soc., Chem. Commun.* **1994**, 1607.

(49) Vogel, E. *Pure Appl. Chem.* **1993**, *65*, 143.

(50) Bondi, A. *J. Phys. Chem.* **1964**, *68*, 441.

shape" adopted by the anthracene moiety in the C_s structure can be defined in terms of the dihedral angles of the central quinone-type ring. The lower vertex C61 is folded down with respect to the plane defined by the four central atoms C62, C63, C65, and C66 by an angle of 42.2° (see Figure 3 for atom numbering). The upper vertex C64 is less folded by an angle of 30.3°. The lateral benzene rings preserve their planarity showing aromatic structures and form an angle of 135.0°.

The energy difference between the perpendicular C_{2v} and the "butterfly-shaped" C_s forms increases to 42.55 kcal/mol for compound **10.** In this case, the folding of the anthracene moiety not only reduces the steric hindrance with the C_{60} cage but also alleviates the nonbonding interactions that take place between the cyano groups and the upper *peri* hydrogens (see Figure 4). As a result, while the lower vertex C61 is folded down by 42.1°, similarly to compound **8**, the upper vertex C64 (36.0°) and the central ring (131.7°) are significantly more bent than in **8.** The folding of the anthracene has been previously discussed for TCNQ derivatives showing that theoretical PM3 predictions are in very good accord with X-ray observations.[51]

For compound **11**, only the "butterfly shaped" structure was calculated. The bending of the anthracene moiety is intermediate between those calculated for **8** and **10**. Folding angles of 42.2° (C61 vertex), 32.9° (C64 vertex), and 133.9° (along the central C61−C64 axis) are found for **11**.

Electronic Structure. The most immediate effect of methano-bridging substitution on the electronic structure of C_{60} is the breaking of the orbital degeneracy associated to the icosahedral symmetry of the ball. As Figure 5a illustrates, the 5-fold degenerate $4h_u$ HOMO of C_{60} calculated at −9.48 eV at the PM3 level splits into five molecular orbitals ranging from −9.75 to −9.32 eV for compound **3a**. Among these five orbitals, only the $31b_1$ HOMO sketched in Figure 5b presents significant contributions from the cyclohexadienone moiety. The orbital displays 2p−π bonding interactions for those bonds exhibiting a higher double-bond character in both the C_{60} cage and the addend. The π-systems of both fragments further overlap giving rise to a through-space bonding interaction that has been previously named as "periconjugation".[19,20]

Periconjugation differs from spiroconjugation in the relative orientations of the atomic orbitals involved in the two interacting π-systems.[19,20] For spiroconjugation, the interacting p_π orbitals lie in parallel planes and give rise to a lateral overlap. For periconjugation, the p_π orbitals lie in perpendicular planes and lead to a more frontal overlap. More intense orbital interactions should therefore be expected for periconjugation. The extension of periconjugation for the HOMO of **3a** is very small since the atomic orbital (AO) coefficients of the C62 and C66 atoms in the LCAO expansion are only 0.05 (see Figure 5), but more effective periconjugative effects are present for lower energy a_2 and b_1 orbitals.

Compared with the parent methanofullerene $C_{60}CH_2$, for which the HOMO is calculated at −9.20 eV, the HOMO of **3a** (−9.32 eV) appears to be 0.12 eV more stable and the HOMO of **6b** (−9.24 eV) is 0.04 eV lower in energy. The greater stabilization found for the HOMO of **3a** should be attributed to periconjugative interactions that transmit the electron-withdrawing inductive effect of the carbonyl group of the addend. Those interactions do not exist for **6** due to the saturated nature of the addend and the inductive effect is more poorly transmitted. The stabilization of the HOMO of **3a** is small because periconjugation is negligible for this orbital and it only exerts an indirect influence through its presence in lower energy orbitals.

(51) Ortí, E.; Viruela, R.; Viruela, P. M. *J. Phys. Chem.* **1996**, *100*, 6138.

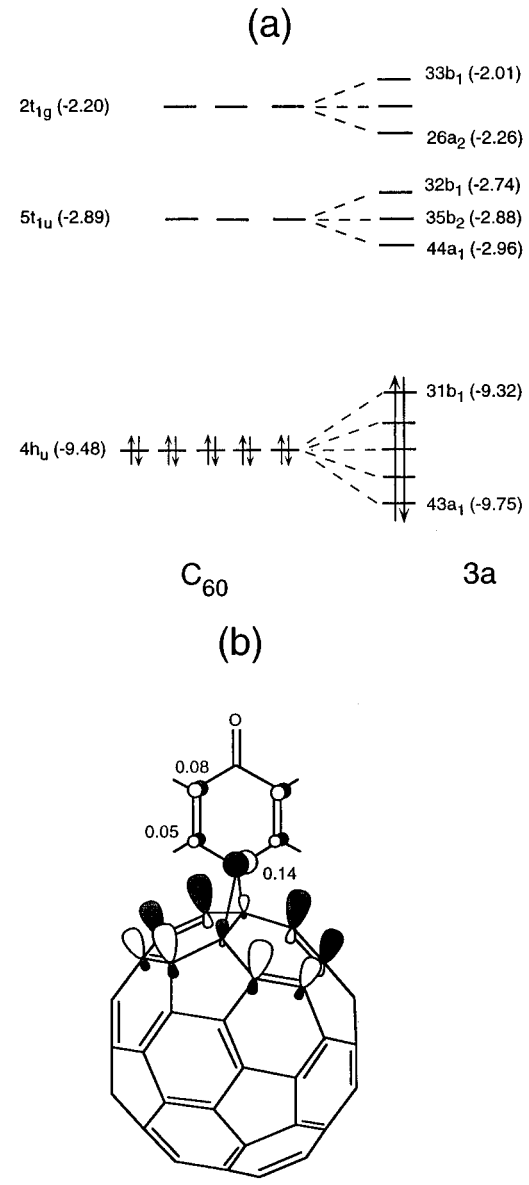

Figure 5. (a) PM3 molecular orbital distributions calculated for C_{60} and **3a**. The energy of the orbitals (in eV) are given within parentheses. (b) Atomic orbital composition of the HOMO of compound **3a**. Coefficients are given for the cyclohexadienone moiety in units of 10^{-2}. Only the contributions of the carbons forming the upper part of C_{60} are given for clarity.

We have calculated the electronic structure of ((3-methylene-1,4-cyclohexadienyl)methano)fullerene (**12**) as a representative example where periconjugation plays an important role in the HOMO. As depicted in Figure 6, the AO contributions of the cyclohexadiene moiety to the HOMO are larger than those obtained for **3a** (cf. Figures 5 and 6) and give rise to an important through-space periconjugation effect. The key for this effect is the fact that the HOMO of the 3-methylene-1,4-cyclohexadiene addend lies at −8.68 eV, i.e. 0.80 eV higher in energy than the HOMO of C_{60} (−9.48 eV) and, therefore, strongly contributes to the HOMO of **12** which appears at −8.98 eV. This is not the case for **3a** because the HOMO of the 1,4-cyclohexadienone addend is calculated lower in energy at −10.19 eV and has a very small contribution to the HOMO of **3a**.

We turn now to analyze the unoccupied orbitals. Methano bridging produces a slight destabilization of the $5t_{1u}$ LUMO of C_{60} which is splitted into three orbitals. The energy of the LUMO seems not to be affected by the size of the addend, since

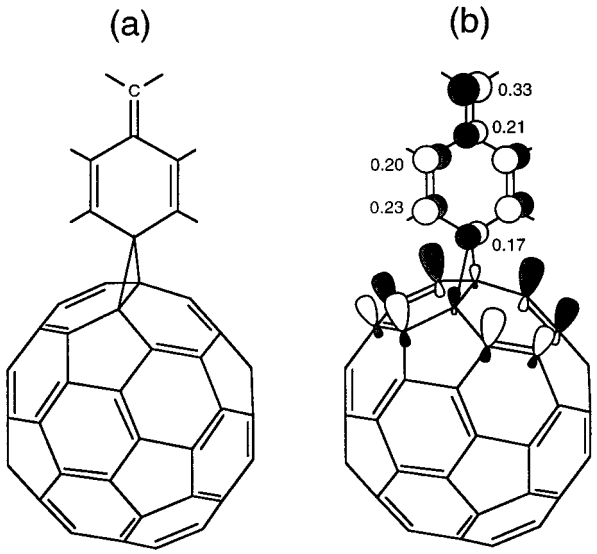

12

Figure 6. (a) Molecular structure of compound **12**. (b) Atomic orbital composition of the HOMO of compound **12**. Coefficients are given for the cyclohexadiene moiety in units of 10^{-2}. Only the contributions of the carbons forming the upper part of C_{60} are given for clarity.

almost identical energies are obtained for the LUMO of C_{60}-CH_2 (−2.82 eV), $C_{60}C_5H_4$ (−2.83 eV), and fluorenofullerene (−2.83 eV). This feature is due to the negligible contribution of the addend to the LUMO. Both the destabilization of the LUMO and the constancy of its energy agree with the experimental CV data reported for methanofullerenes. The former explains the slightly more negative first-reduction potentials measured for (diphenylmethano)fullerene (−1.18 V) and fluorenofullerene (−1.175 V) compared with the parent C_{60} (−1.123 V).[19] The latter justifies the almost identical values of those potentials.

The attachment of the cyclohexadienone moiety to C_{60} places the LUMO of **3a** 0.07 eV below the LUMO of C_{60} (see Figure 5). This result agrees with the more electronegative character found for **3a**, for which the first-reduction potential is anodically shifted with respect to C_{60} (see Table 1). Although the through-space periconjugation interaction plays no direct role on the LUMO of **3a**, since the 2p−π orbitals of the cyclohexadienone unit do not contribute to this orbital, its occurrence in lower energy orbitals transmit the inductive effect of the addend and produces a small stabilization of all the orbitals localized on the C_{60} cage. Compared to $C_{60}CH_2$, the LUMO of **3a** is stabilized 0.14 eV similarly to that found for the HOMO.

The reason for the total absence of periconjugation in the LUMO of **3a** is that the LUMO of the addend, calculated at −0.47 eV, lies very high in energy with respect to the LUMO of C_{60} (−2.89 eV), and there is no effective overlap between the LUMOs of both fragments. To investigate the effect of more electronegative addends, we calculated the electronic structure of the TCNQ analogue of **3a** resulting from the substitution of the oxygen atom by a $C(CN)_2$ group. The synthesis of this compound was in fact intended by condensation of malononitrile with **3a,** but the reaction did not work as discussed above. Although the LUMO of the addend now lies at −1.64 eV, it is still 1.25 eV above the LUMO of C_{60} and has no contribution to the LUMO of the adduct which now appears at −3.02 eV, i.e. only 0.06 eV lower in energy than for **3a**. The TCNQ analogue of **3a** would therefore show a first-reduction potential only slightly less negative than that measured for **3a**.

The effect of periconjugation on the energy of the LUMO and thereby on the reduction potentials of spiroannelated methanofullerenes such as **3a** and its TCNQ analogue is small because it only plays the indirect role of transmitting the inductive effect of the electronegative addend. We believe, however, that periconjugation can be used to obtain fullerenes with more significantly improved acceptor properties. The challenge is to synthesize methanofullerenes with conjugated addends showing a more electronegative character, in such a way that their LUMO would lie close in energy or even below the LUMO of C_{60} and an effective periconjugative interaction would take place between the LUMOs of both fragments. Periconjugation would therefore play a direct role in determining the energy of the LUMO of the adduct and would lead to methanofullerenes with significantly enhanced electron-acceptor properties.

PM3 calculations indicate that the LUMO, LUMO+1, and LUMO+2 orbitals of **8** lie at almost the same energies than for **3a** when the anthraquinone moiety is forced to be perpendicular to the C1−C2 bond (C_{2v} structure). These orbitals are, however, destabilized by ∼0.12 eV when the addend adopts the more stable butterfly structure due to the loss of periconjugative interactions (see Figure 4). The LUMO of **8** (−2.84 eV) therefore appears at slightly higher energies than the LUMO of C_{60} (−2.89 eV), thus supporting the shift of 0.09 V to more negative values experimentally observed for the first-reduction potential of **8.** The more electronegative character of the $C(CN)_2$ and N−CN groups determines that the LUMOs calculated for the folded structures of **10** (−2.89 eV) and **11** (−2.88 eV) lie at almost the same energies than for C_{60}. This result explains the almost identical values measured for the first-reduction potentials of C_{60}, **10**, and **11** (see Table 1).

Since the energies of the unoccupied orbitals strongly depend on the theoretical approach, the electronic structure of **3a** was further investigated by performing single-point calculations on the PM3-optimized geometries of C_{60}, $C_{60}CH_2$, and **3a** at the DFT level using the hybrid gradient-corrected B3P86 density functional[52] and the 3-21G basis set[53] and at the ab initio HF level using the more extended 6-31G* basis set.[54] The molecular orbital descriptions provided by both approaches are identical with those obtained from the PM3 results. At the B3P86/3-21G level, the LUMO of **3a** lies 0.10 eV below the LUMO of C_{60} and 0.18 eV below the LUMO of $C_{60}H_2$. At the HF/6-31G* level, these relative energies increase to 0.20 and 0.25 eV, respectively. These results support the predictions performed above on the basis of PM3 calculations.

Reduced Compounds. Compound **3a** was chosen as a representative example to investigate the reduction process. The geometric structure of the anion of **3a** was first optimized at the PM3 level using the restricted open-shell Hartree−Fock (ROHF) formalism.[55] Two possible structures were considered for $\mathbf{3a}^{\bullet-}$: a closed C_{2v} structure similar to that depicted in Figure 3 for the neutral compound and an open structure where the cyclopropane C2−C61 bond is broken. The opening of the

(52) The B3P86 functional consists of Becke's three-parameter hybrid functional,[52a] which is a hybrid of Hartree−Fock exchange with local and gradient-corrected exchange and correlation terms, with the nonlocal correlation provided by the "Perdew 86" [52b] expression. (a) Becke, A. D. *J. Chem. Phys.* **1993,** *98*, 5648. (b) Perdew, J. P. *Phys. Rev. B* **1986**, *33*, 8822.

(53) Binkley, J. S.; Pople, J. A.;, Hehre, W. J. *J. Am. Chem. Soc.* **1980**, *102*, 939. Gordon, M. S.; Binkley, J. S.; Pople, J. A.; Pietro, W. J.; Hehre, W. J. *J. Am. Chem. Soc.* **1982**, *104*, 2797. Pietro, W. J.; Francl, M. M.; Hehre, W. J.; DeFrees, D. J.; Pople, J. A.; Binkley, J. S. *J. Am. Chem. Soc.* **1982**, *104*, 5039.

(54) Hariharan, P. C.; Pople, J. A. *Chem. Phys. Lett.* **1972**, *16*, 217.

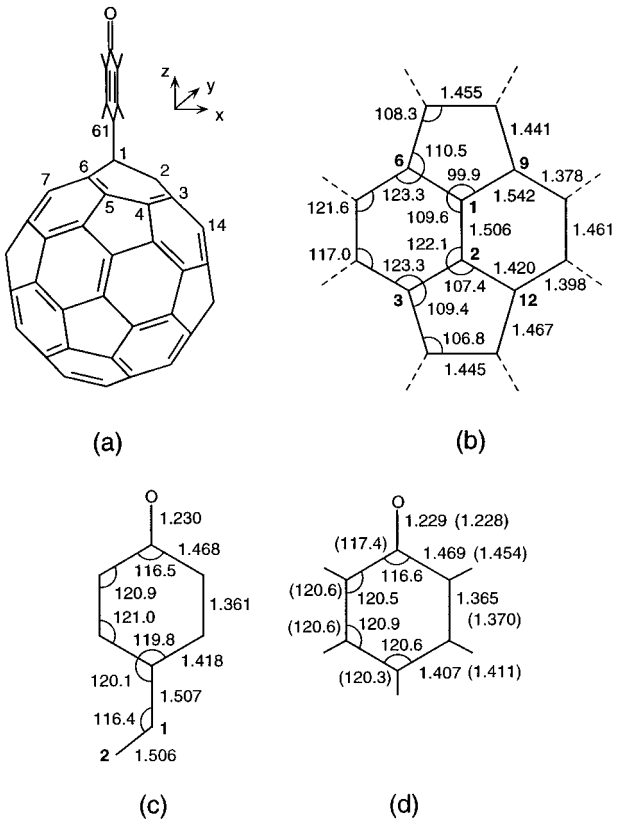

Figure 7. (a) PM3-optimized geometry calculated for the open-cyclopropane structure of **3a**$^{\bullet-}$. The atom numbering and axis orientation are the same as those used in Figure 3. (b) Geometry of the pyracylene unit around the C1−C2 bond. (c) Geometry of the cyclohexadienone moiety. The optimizing geometry is symmetric with respect to the *xz* plane passing through the C1−C2 bond. (d) PM3 bond lengths and bond angles calculated for the phenoxyl radical (CASSCF values from ref 58 are given within parentheses). Bond lengths are in angstroms and bond angles in degrees.

cyclopropane ring was first suggested for methanofullerenes bearing electronegative addends such as fluorenofullerenes with electron-withdrawing groups[19] and has been invoked as a possible reason to explain the irreversible electrochemical behavior observed for the quinone-type derivatives **3**, **8**, **10**, and **11**.

The geometry calculated for the closed C_{2v} structure of **3a**$^{\bullet-}$ is almost identical with that obtained for the neutral molecule. This result agrees with the small changes observed with respect to C_{60} in the geometry of low-charged alkali-metal fullerides.[56] The PM3-optimized geometry obtained for the open structure is sketched in Figure 7. It is symmetric with respect to the *xz* plane containing the C1−C2 bond thus presenting a C_s symmetry. The opening of the cyclopropane ring produces important asymmetries in the neighborhood of the transannular C1−C2 bond (cf. Figures 3b and 7b), which now has a length of 1.506 Å. While the C1−C6 and C1−C9 bonds lengthen to 1.542 Å, the C2−C3 bond and C2−C12 bonds shorten to 1.420 Å. While the bond angles surrounding the C1 atom narrow to 99.9 and 109.6°, those encircling the C2 atom widen to 107.4 and 122.1°. These changes reflect the large sp^3 character of the C1 atom that largely protrudes from the C_{60} skeleton (see Figure 7a). The pentagon and the two hexagons delimiting the C1 vertex are folded up along the respective C6−C9, C2−C6, and C2−C9 axes by ∼15−17°.

The PM3 method predicts that the open-cyclopropane C_s structure is more stable than the closed-cyclopropane C_{2v} structure by an energy difference of 4.03 kcal/mol. To ascertain the reliability of this result, the PM3-optimized geometries of both structures were recalculated, in a first step, at the DFT B3P86/3-21G level. These calculations confirm the PM3 result and reduce the energy difference between open and closed structures to 2.05 kcal/mol. In a second step, the geometries of both structures were reoptimized at the DFT B3P86/3-21G level and at the ab initio HF/6-31G* level. Both approaches predict the open structure to be more stable by 2.40 and 4.33 kcal/mol, respectively.[57] These results support the PM3 predictions and point out that the energy difference between the open and closed structures of **3a**$^{\bullet-}$ is on the order of a few kilocalories per mole. The greater stability of the open structure is experimentally confirmed on the basis of ESR measurements as discussed below.

Table 2 summarizes the B3P86/3-21G and HF/6-31G* net atomic charges and spin densities calculated for the cyclohexadienone moiety of neutral **3a** and its anion. In both cases, the charge distribution remains almost unchanged in passing from **3a** to **3a**$^{\bullet-}$, showing that the extra electron enters the C_{60} cage for both the closed and the open structures of the anion. This is an expected result since the LUMO, i.e., the orbital which accepts the extra electron, of **3a** belongs to the C_{60} cage with almost no contribution from the addend. The total charge accumulated by the cyclohexadienone moiety is thus almost zero for both structures of **3a**$^{\bullet-}$ as it is also for neutral **3a**.

The calculated spin densities show that, for the closed structure, the unpaired electron is delocalized on the C_{60} backbone and there is no spin density on the cyclohexadienone moiety. The opposite is found for the open structure, for which spin densities are zero for C_{60} and the unpaired electron resides on the addend. This indicates that the extra electron causes the homolytic breaking of the C2−C61 bond and, as a consequence, the C_{60} cage has a paired number of electrons and a negative charge, while the cyclohexadienone moiety accommodates the unpaired electron and gives rise to a phenoxyl radical. The opening of the cyclopropane structure is schematically shown on the left part of Figure 8. The spin densities calculated for open structure of **3a**$^{\bullet-}$ also indicate that the unpaired electron is highly delocalized on the resulting phenoxyl radical. Maximum spin densities are found for C61, C63, C65, and the oxygen atom, while they are almost zero for C62, C64, and C66. These densities agree with the resonance structures depicted on the right part of Figure 8.

The opening of the cyclopropane ring induces important changes on the geometry of the cyclohexadienone moiety (cf. Figures 3c and 7c). The C═O bond is 0.012 Å longer and the adjacent C−C bonds are 0.015 Å shorter than in neutral **3a**. The C62−C63 and C65−C66 bonds (1.361 Å) are now intermediate between the 1.335 Å distance found in *p*-benzoquinone and the 1.397 Å distance in benzene. The C61−C62

(55) The ROHF formalism was used instead of the more appropriate spin-unrestricted UHF formalism owing to the high spin contamination obtained for the open structure of **3a**$^{\bullet-}$ ($\langle S^2\rangle = 3.3$ as compared to 0.75 for a pure doublet state), which makes the energy comparison with the noncontaminated closed structure meaningless. Exploratory calculations for the open structure of **3a**$^{\bullet-}$ at the ab initio UHF/3-21G* and 6-31G* levels also lead to high spin contaminations ($\langle S^2\rangle \approx 2.0$). This problem has been discussed for open-shell fullerenes by Thiel et al. (ref 43d), who also adopted the ROHF treatment.

(56) Zhou, O.; Cox, D. E. *J. Phys. Chem. Solids* **1992**, *53*, 1373. Rosseinsky, M. J. *J. Mater. Chem.* **1995**, *5*, 1497.

(57) B3P86/3-21G and HF/6-31G* calculations were performed using the ROHF formalism and a tight convergence criterion of 10^{-8} for the density matrix. Although this criterion makes each calculation very costly in computer time (at the HF/6-31G* level, each optimization cycle of the open C_s structure of **3a**$^{\bullet-}$ took about 40 h on a Silicon Graphics Power Challenge XL-R8000/90 computer), lower convergence criterions should not be used due to the large size of the molecule.

Table 2. Net Atomic Charges and Spin Densities Calculated at the B3P86/3-21G and the HF/6-31G* (within parentheses) Levels for the Cyclohexadienone Moiety of Neutral **3a** and Its Anion (Both Closed- and Open-Cyclopropane Structures Are Given for **3a**$^{\bullet-}$)[a]

	net charges			spin densities	
atom[b,c]	**3a**	**3a**$^{\bullet-}$ (closed)	**3a**$^{\bullet-}$ (open)	**3a**$^{\bullet-}$ (closed)	**3a**$^{\bullet-}$ (open)
C61	−0.17 (−0.04)	−0.19 (−0.07)	0.16 (0.10)	0.00 (0.00)	0.24 (0.35)
C62 (C66)	−0.14 (−0.12)	−0.13 (−0.10)	−0.21 (−0.19)	0.00 (0.00)	0.01 (0.02)
C63 (C65)	−0.23 (−0.28)	−0.24 (−0.30)	−0.23 (−0.26)	0.00 (0.00)	0.17 (0.18)
C64	0.39 (0.53)	0.38 (0.53)	0.36 (0.50)	0.00 (0.00)	0.03 (0.07)
O	−0.48 (0.57)	−0.51 (−0.60)	−0.51 (−0.62)	0.00 (0.00)	0.28 (0.17)
H62 (H66)	0.25 (0.24)	0.25 (0.24)	0.24 (0.23)	0.00 (0.00)	0.00 (0.00)
H63 (H65)	0.25 (0.24)	0.23 (0.21)	0.22 (0.21)	0.00 (0.00)	0.00 (0.00)
Q[d]	−0.01 (0.06)	−0.11 (−0.04)	0.04 (−0.03)		

[a] The calculations on the anion were performed within the spin-restricted HF formalism using a spin multiplicity value of 2. [b] See Figure 3a for atom numbering. [c] The C_{2v} symmetry is lost for the open-cyclopropame structure of **3a**$^{\bullet-}$. [d] *Q* denotes the total net charge accumulated by the cyclohexadienone moiety.

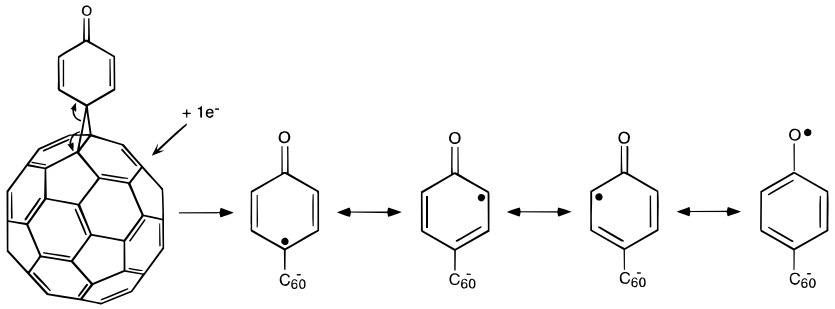

Figure 8. Homolytic breaking of the C2−C61 bond of **3a** upon reduction and resonance structures of the resulting phenoxyl radical.

and C1−C66 bonds (1.418 Å) are only 0.021 Å longer than the C−C bonds in benzene and considerably shorter than in *p*-benzoquinone. The opening of the cyclopropane structure thus causes a partial aromatization of the cyclohexadienone moiety. While the C═O environment resembles the quinoid structure of *p*-benzoquinone, the C61 vicinity is similar to the aromatic structure of benzene. The predicted geometry actually corresponds to that of the phenoxyl radical (cf. Figure 7c,d). Figure 7d further compares the PM3 geometry obtained for the phenoxyl radical with that obtained from very accurate CASSCF calculations.[58] Both geometries show a good correlation, thus proving the reliability of the PM3-optimized geometries.[59]

We believe that the possibility of delocalizing the unpaired electron within the addend, together with the aromatization of the geometry of the addend are the factors which determine the opening of the cyclopropane ring for methanofullerenes since both factors contribute to the stabilization of the open-cyclopropane structure. Two requirements are therefore necessary for the opening of the methanofullerene: (i) the addend should be a conjugated system that allows for the delocalization of the unpaired electron, and (ii) the addend should gain in aromaticity when the cyclopropane ring is open. These two requirements are fulfilled by the quinone-type derivatives **3** and, in a lower degree, by **8**, **10**, and **11**, because the anthrone-type addend in these compounds is highly distorted from planarity. This is not the case for the nonconjugated derivative **6b**, for which there is no possibility of delocalizing the unpaired electron on the addend, and the reduction process will occur via a closed structure.

Work in progress, involving in situ reduction of compound **3c** in the CW-ESR cavity, has demonstrated that indeed ring opening occurs as predicted by theoretical calculations.[60] During the chemical reduction of **3c**, with decamethylnickelocene, $Ni(C_5Me_5)_2$, in benzonitrile,[61] a transient ESR structurated signal (Figure 9) was observed. This signal appears at $g = 2.0030$, which is very similar to those reported for some substituted 2,6-dimethylphenoxyl radicals[62] and is much larger than that of radical anion derived from C_{60} ($g = 1.9999$).[63] In addition, the hyperfine structure of this signal can be simulated by the coupling of the unpaired electron with six equivalent hydrogen atoms of two methyl groups with a coupling constant of 1.0 G and a line width of 1.2 G.[64] Consequently, this rather unstable species can be adscribed to **3c**$^{\bullet-}$, confirming, therefore,

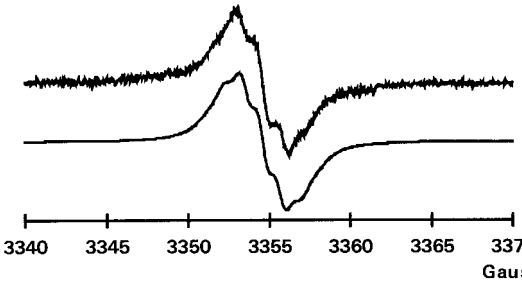

Figure 9. ESR spectra of reduced **3c**: (upper trace) experimental spectrum in benzonitrile at 260 K; (lower trace) simulated spectrum using the values given in the text.

(58) Chipman, D. M.; Liu, R.; Zhou, X.; Pulay, P. *J. Chem. Phys.* **1994**, *100*, 5023. Quin, Y.; Wheeler, R. A. *J. Chem. Phys.* **1995**, *102*, 1689.

(59) The averaged difference between the geometric parameters calculated for the phenoxyl radical at the ROHF-PM3 level and the CASSCF geometry given in ref 58 is only 0.006 Å for the bond lengths and 0.4° for the bond angles.

(60) The poor solubility of **3c** in most solvents, as well as the transient character of its reduced species, prevents at our hands the ESR study of the reduction process by coulombimetry. Nevertheless, in situ chemical reduction of **3c** was accomplished by using decamethylnickelocene, $Ni(C_5Me_5)_2$, in benzonitrile as a reducing agent (ref 61).

(61) Decamethylnickelocene is a selective reductant ($E_{1/2}^{+/0} = -0.65$ V vs SCE) for the production of radical anion of C_{60}, see: Wan, W. C.; Liu, X.; Sweeney, M.; Broderick, W. E. *J. Am. Chem. Soc.* **1995**, *117*, 9580.

(62) For ESR parameters of some substituted 2,6-dimethylphenoxyl radicals, see: Landolt-Börnstein, New Series **1986**, *11/17e*, 206 and references therein.

(63) Khaled, M. M.; Carlin, R. T.; Turlove, P. C.; Eaton, G. R.; Eaton, S. S. *J. Am. Chem. Soc.* **1994**, *116*, 3465.

(64) The poor resolution of the obtained spectrum prevents to give by simulation a reliable value for the coupling constant of the two aromatic hydrogen atoms of **3c**$^{\bullet-}$.

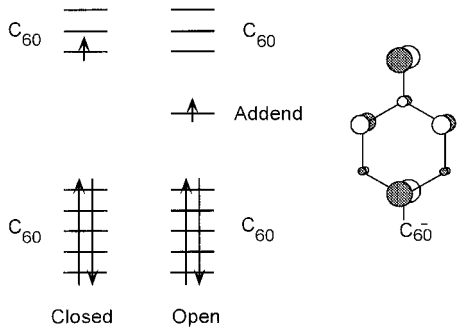

Figure 10. Schematic diagram showing the molecular orbital distributions calculated for the closed- and open-cyclopropane structures of **3a**$^{\bullet-}$. The molecular units (C_{60} or addend) to which the orbitals belong are indicated on one side. The atomic orbital composition of the semioccupied orbital of the open structure is depicted on the right.

the theoretical prediction that the unpaired electron of **3a**$^{\bullet-}$ resides mainly at the addend and the negative charge on the ball.

Figure 10 illustrates the molecular orbital (MO) distribution obtained for the closed- and open-cyclopropane structures of **3a**$^{\bullet-}$. For the closed structure, the MO ordering is identical with that depicted in Figure 5a for the neutral molecule and the unpaired electron lies in one of the three almost degenerate LUMOs localized on the C_{60} cage. The second, third, and fourth electrons are therefore expected to occupy these orbitals and enter the C_{60} ball. This explains the fact that the cyclic voltammogram of the cyclohexanone derivative **6b**, for which the closed structure should be favored, presents well-resolved reversible reduction waves at reduction potentials similar to those of the parent C_{60} (see Figure 2b and Table 1).

For the open structure, a new orbital localized on the quinone-type addend appears between the HOMOs and the LUMOs of the C_{60} cage as a consequence of the structural changes. This orbital corresponds to the semioccupied HOMO of the phenoxyl radical, and its AO composition reflects the mixed aromatic-quinoid character of this radical (see Figure 10). The second electron in **3a**, for which the open structure is energetically favored, is therefore expected to enter in the addend, thus completing the HOMO of the phenoxyl radical. This result completely explains the electrochemical properties recorded for compounds **3**. The fact that the first-reduction wave in the CV curve of **3b** corresponds to a two-electron process and in **3c** presents a shoulder at −1197 mV are therefore due to the attachment of the second electron to the addend. In this way, both the C_{60} cage and the addend bear a negative charge for **3a**$^{2-}$. The third and fourth electrons in the reduction process will be accommodated in the LUMOs of C_{60} and the respective reduction waves (−1620 and −2037 mV for **3b** and −1602 and −2016 mV for **3c**) correspond to the second (−1455 mV) and third (−1913 mV) reduction processes in C_{60}.

To give a further insight into the reduction process, the closed- and open-cyclopropane structures of **3a**$^{2-}$ were first optimized at the PM3 and calculated at the B3P86/3-21G level and second reoptimized at the ab initio HF/6-31G* level. The atomic charge distributions confirm that the second electron enters in the C_{60} cage for the closed structure, while it is accommodated by the addend for the open structure. The open structure of **3a**$^{2-}$ is calculated to be more stable than the closed structure by 15.94 kcal/mol at the PM3 level and by 11.26 kcal/mol at the B3P86/3-21G level.[65] The energy difference increases to 33.54 kcal/mol when the geometries were optimized at the HF/6-31G* level. The greater stability of the open structure explains the collapse of the first- and second-reduction processes under the first CV reduction wave, since the two electrons reside on different sites.

Although the nature of the addend in compounds **8**, **10**, and **11** is of quinone-type, the electrochemical properties of these methanofullerenes differ from those of **3**. The first-reduction process in **8**, **10**, and **11** is well-separated from the second reduction, and several reductions processes appear now at close potentials in the zone −1300 to −1600 mV. To explain this electrochemical behavior, the geometries of the anion and dianion of **10** were optimized at the PM3 level. Although the calculations performed for the anion were not conclusive, since it was impossible to reduce the gradient norm for the open-cyclopropane structure below a value of 13 au, they clearly indicate that the closed-cyclopropane structure is more stable than the open structure for **10**$^{\bullet-}$. The calculations performed for the dianion predict that the open structure is more stable than the closed structure by 15.91 kcal/mol, similarly to that found for **3a**. These results suggest that the second electron enters the ball and induces the heterolytic breaking of the C2−C61 bond since both the C_{60} cage and the addend are found to bear a negative charge in the resulting open structure. The result of the reduction process, even the opening of the cyclopropane ring takes place by different ways, is thus the same for **3** and **10** since, after the entrance of the two first electrons, both the ball and the addend are reduced.

The calculations on **10**$^{2-}$ illustrate that the addend in the more stable open structure, although less folded than in neutral **10**, remains significantly distorted from planarity. The absence of planarity reduces the gain of aromaticity when the electron is attached to the addend and therefore shifts the reduction potential associated to that attachment to more negative voltages compared to **3**. This shifting has been experimentally observed for TCNQ and DCNQI benzoannulated derivatives[66] and explains the appearance of the second reduction potential of the anthraquinone-type derivatives **8**, **10**, and **11** at more negative potentials than in **3**, in the zone of the second-reduction wave of C_{60} (see Table 1).

It is difficult to unambiguously assign the reduction potentials of these compounds to specific electron attachments with the exception of the first electron that always enters the C_{60} cage. We believe that the second-reduction potential in **10** (−1383 mV) and **11** (−1321 mV) corresponds to the attachment of the electron to the addend. The reduction potential is slightly less negative for **11** because the addend is less distorted from planarity. In this way, the reduction potentials at −1537 mV (**10**) and −1536 mV (**11**) would correspond to the second reduction of the ball. For compound **8**, the reduction of the addend is shifted to more negative potentials due to the lower electronegative character of the C═O group compared with the $C(CN)_2$ and N−CN groups. It is therefore very difficult to distinguish which of the two potentials at −1525 and −1670 mV corresponds to the reduction of the addend and which is due to the second reduction of C_{60}.

Synopsis. The synthesis of new methanofullerenes bearing quinone-type addends including TCNQ and DCNQI analogues has been described. Compared to C_{60}, the methanofullerenes exhibit irreversible CV curves with additional reduction peaks. Only the nonconjugated cyclohexanone derivative **6** shows an electrochemical behavior with reversible reduction waves cor-

(65) The closed and open PM3 structures of **3a**$^{2-}$ were also calculated at the B3P86/6-31G* level obtaining an energy difference of 10.48 kcal/mol. These calculations were not feasible for **3a**$^{\bullet-}$ owing to the impossibility of converging the closed structure.

(66) Aumüller, A.; Hünig, S. *Liebigs Ann. Chem.* **1984**, 618. Kini, A. M.; Cowan, D. O.; Gerson, F.; Möckel, R. *J. Am. Chem. Soc.* **1985**, *107*, 556. Aumüller, A.; Hünig, S. *Liebigs Ann. Chem.* **1986**, 165.

responding to those of C_{60}. The conjugated cyclohexadienone derivatives **3** exhibit better acceptor properties than C_{60}.

Semiempirical PM3 calculations show that the cyclohexadienone addend in **3** lies perpendicular to the transannular bond. This perpendicularity is however lost for compounds **8**, **10**, and **11** due to the interactions of the *peri* hydrogens of the anthrone-type addend with the C_{60} backbone. To minimize these interactions the addend loses the planarity and adopts a "butterfly shaped" structure.

From the electronic structure standpoint, methano bridging breaks the orbital degeneracy of C_{60} and produces a slight destabilization of the LUMO. This explains the shifting to more negative values of the reduction potentials of "standard" methanofullerenes such as **6**. For compounds **3**, the pericon-jugative interactions between the π-systems of the addend and the C_{60} ball help to transmit the electron-withdrawing inductive effect of the addend and produce a small stabilization of the orbitals of C_{60}. This justifies the slightly less negative first-reduction potentials measured for **3** compared to C_{60}. Compounds **8**, **10**, and **11** present reduction potentials similar to those of C_{60} due to the disappearance of periconjugative effects as a consequence of the folding of the addend.

The first electron in the reduction process always enters the C_{60} ball. Semiempirical (PM3), DFT (B3P86/3-21G), and ab initio (HF/6-31G*) calculations indicate that, for compounds **3**, the attachment of the electron causes the homolytic breaking of one of the bonds connecting the addend to C_{60}. The resulting open-cyclopropane structure is stabilized by the delocalization of the unpaired electron on the addend, which gains in aromaticity and presents a phenoxyl radical structure. ESR spectroscopy provides experimental evidence for such unpaired electron delocalization. The second electron in the reduction process therefore enters in the addend. The opening of the cyclopropane structure thus explains the irreversible electrochemical behavior observed for compounds **3**, for which the first-reduction wave, which involves two electrons, implies the reduction of both the ball and the addend. For compound **6**, the nonconjugated nature of the addend determines that the reduction process goes via a closed-cyclopropane structure. The first electrons thus enter in the unoccupied orbitals of the ball, explaining the similar electrochemical behavior observed for **6** and C_{60}.

The reduction process in compounds **8**, **10**, and **11** also proceeds via an open-cyclopropane structure, but this structure is now obtained after the attachment of the second electron which produces the heterolytic opening of the cyclopropane ring. The second-reduction process thus corresponds to the reduction of the addend as for **3** but is shifted to more negative potentials due to the nonplanar structures of the addends that reduce the gain of aromaticity.

Experimental Section

Spiro[10-dicyanomethylenanthrone-9,61′-methanofullerene] (10). To a solution of the spiro[C_{60}-anthrone] (**8**) (130 mg, 0.142 mmol) in dry chloroform (100 mL) was added $TiCl_4$ (1 M solution in CH_2Cl_2) (71.1 mg, 0.375 mmol), and a brown suspension was formed. Then, a solution of malononitrile (50 mg, 0.75 mmol) and pyridine (0.125 mL) in dry chloroform (3 mL) was added. The reaction mixture was stirred at reflux temperature overnight, new amounts of $TiCl_4$ (142.2 mg, 0.75 mmol), malononitrile (100 mg, 1.50 mmol), and pyridine (0.250 mL) were added, and the reaction mixture was refluxed for an additional 13 days (monitored by TLC). The reaction mixture was concentrated and submitted to flash chromatography (SiO_2, toluene) to give 35 mg of brown pure compound (26% yield) (37% based on consumed starting material). ^{1}H NMR (CS_2/500 MHz): 8.28 (m, 2H), 8.08 (m, 2H), 7.60−7.55 (m, 4H). FTIR (KBr): 2223 (CN) (w), 1598 (m), 1586 (m), 1464 (m), 1452 (m), 1428 (m), 1187 (m), 780 (m), 768 (m), 753 (m), 701 (m), 556 (m), 527 (s) cm^{-1}. FABMS (*o*-dichlorobenzene/NBA): *m*/*z* 961 $(M + H)^{+\cdot}$ 920, 767, 748, 720-(C_{60}). Anal. Calcd for $C_{77}H_8N_2$: C, 96.25; H, 0.83; N, 2.91. Found: C, 96.01; H, 1.01; N, 3.03. UV−vis (toluene) λ_{max} (nm): 286, 330, 434, 492, 694.

Spiro[10-cyanoiminoanthrone-9,61′-methanofullerene] (11). To a solution of the spiro[C_{60}-anthrone] (**8**) (91.2 mg, 0.10 mmol) in dry chloroform (80 mL) was added $TiCl_4$ (1M solution in CH_2Cl_2) (189.7 mg, 1 mmol), and a brown suspension was formed. Then bis-(trimethylsilyl)carbodiimide (BTC) (1.09 mL, 5 mmol) was added dropwise, and the resulting black solution was stirred at reflux temperature overnight. New amounts of $TiCl_4$ and BTC were added, and the reaction mixture was refluxed for additional 5 days. After this time, all the starting material was exhausted (monitored by TLC). The reaction mixture was concentrated and submitted to flash chromatography (SiO_2, toluene) to give 55 mg of brown pure compound (60% yield). ^{1}H NMR (CS_2/500 MHz): 8.65 (dd, J = 12, 2.0 Hz, 1H), 8.40 (dd, J = 11, 2.0 Hz, 1H), 8.33 (d, J = 14, 1H), 8.10 (d, J = 13, 1H) 7.65−7.50 (m, 4H). FTIR (KBr): 2171 (CN) (m), 1608 (s), 1589 (s), 1568 (s), 1464 (m), 784 (m), 587 (m), 556 (m), 527 (s) cm^{-1}. FABMS (chloroform/NBA): *m*/*z* 937 $(M + H)^+$, 766, 746, 720 (C_{60}). HRMS: calcd for $C_{75}H_8N_2$ $(M + H)^+$ 937.0766, found 937.0762. Anal. Calcd for $C_{75}H_8N_2$: C, 96.15; H, 0.85; N, 2.99. Found: C, 95.87; H, 1.04; N, 3.01. UV−vis (toluene) λ_{max} (nm): 282, 330, 410 (sh), 435, 498, 698.

Acknowledgment. We are grateful to the National Science Foundation for support through Grant DMR 95-00888. The groups from Valencia and Madrid jointly acknowledge the DGICYT Grant PB95-0428-CO2. The research performed by the group at the University of Valencia was also supported by the CICYT Grants MAT95-1630-E and IN95-0326. This group thanks Professor F. Tomás for his valuable support and W. Díaz for his technical assistance. The work performed by the group in Barcelona was supported by the CICYT (Grant MAT94-0797) and CIRIT (Grant SGR 95/00507) agencies.

Supporting Information Available: Table S1 (containing experimental conditions for mono adducts **8** and bis adducts **9**), Table S2 (containing PM3-optimized geometries of the cyclopropane environment in **3a**, **6b**, **8**, **10**, **11**, $C_{60}CH_2$, and $C_{60}C_5H_4$), and part of the Experimental Section (containing the synthesis and spectroscopic characterization of compounds **4**, **5a,b**, **6a,b**, and **9**) (6 pages). See any current masthead page for ordering and Internet access instructions.

JA962299K